Title
Feasibility of Infrared Imaging Arrays Using High T{sub c} Superconducting Bolometers

Journal
Journal of Applied Physics, 71(6)

Authors
Verghese, S.
Richards, P.L.
Char, K.
et al.

Publication Date
1991-10-01

LBL-31411
Preprint

Center for Advanced Materials

CAM

Submitted to Journal of Applied Physics

Feasibility of Infrared Imaging Arrays Using High T_c Superconducting Bolometers

S. Verghese, P.L. Richards, K. Char, D.K. Fork, and T.H. Geballe

October 1991

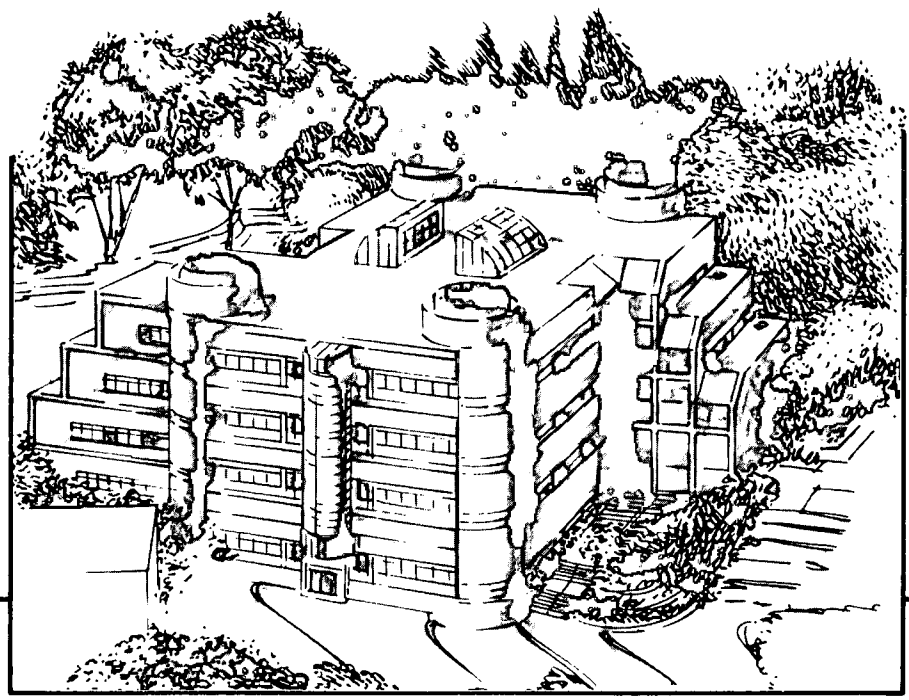

Materials and Chemical Sciences Division

Lawrence Berkeley Laboratory • University of California

ONE CYCLOTRON ROAD, BERKELEY, CA 94720 • (415) 486-4755

Prepared for the U.S. Department of Energy under Contract DE-AC03-76SF00098

DISCLAIMER

LBL-31411

Feasibility of infrared imaging arrays using high T_c superconducting bolometers

S. Verghese and P. L. Richards

Department of Physics, University of California and
Materials Sciences Division, Lawrence Berkeley Laboratory,
Berkeley, CA 94720.

K. Char

Conductus Inc., Sunnyvale CA 94086.

D. K. Fork

Xerox Palo Alto Research Center, Palo Alto, CA 94304 and
Department of Applied Physics, Stanford University, Stanford, CA 94305.

T. H. Geballe

Department of Applied Physics, Stanford University, Stanford, CA 94305.

This work was supported in part by the Director, Office of Energy Research, Office of Basic Energy Sciences, Materials Sciences Division of the U.S. Department of Energy under Contract No. DE-AC03-76SF00098 (for SV, PLR), by Conductus Inc. (for KC), by the Air Force Office of Scientific Research (AFOSR) under Contract No. F49620-89-C-0017 (for DKF, THG), and by Xerox Palo Alto Research Center (for DKF). SV acknowledges a Department of Education predoctoral fellowship. DKF acknowledges an ATT predoctoral fellowship.

Feasibility of infrared imaging arrays using high T_c superconducting bolometers

S. Verghese and P. L. Richards

Department of Physics, University of California and
Materials Sciences Division, Lawrence Berkeley Laboratory,
Berkeley, CA 94720.

K. Char

Conductus Inc., Sunnyvale CA 94086.

D. K. Fork

Xerox Palo Alto Research Center, Palo Alto, CA 94304 and
Department of Applied Physics, Stanford University, Stanford, CA 94305.

T. H. Geballe

Department of Applied Physics, Stanford University, Stanford, CA 94305.

ABSTRACT

We discuss the design of high T_c superconducting bolometers for applications such as infrared imaging arrays. The dependence of bolometer sensitivity on excess voltage noise in the thermometer is a function of the detector area and thus of the wavelength to be detected. We use measurements of the voltage noise in thin films of $YBa_2Cu_3O_{7-\delta}$ on Si, Si_3N_4, and sapphire substrates to predict the performance of different bolometer architectures. Useful opportunities exist for bolometers made on both Si and Si_3N_4 membranes. We also describe a readout scheme for two dimensional arrays of bolometers in which real-time signal integration is performed on the chip.

INTRODUCTION

Much recent work has focused on the high T_c superconducting bolometer as an infrared detector.[1-9] Such bolometers consist of an infrared radiation absorber thermally coupled to a high T_c superconducting thermometer operated at its resistive transition, both weakly coupled to a liquid nitrogen cooled heat sink at 77 K. For the purposes of this paper we consider only relatively sensitive slow composite bolometers that absorb radiation directly and are constructed on thin substrates that are thermally isolated from the heat sink. We will not consider the fast bolometers obtained when a high T_c film is deposited directly on a bulk substrate[10-13] or the antenna-coupled microbolometer.[14, 15]

For wavelengths $\lambda < 20\,\mu$m, photovoltaic infrared detectors such as HgCdTe give excellent performance at 77K. For wavelengths $\lambda > 20\,\mu$m, the sensitivity of semiconducting detectors at or above 77K is poor and room temperature thermal detectors such as the pyroelectric detector, the thermopile, or the Golay cell are used in applications where a liquid nitrogen-cooled high T_c bolometer could be conveniently used. The high T_c bolometer offers higher sensitivity under these conditions, primarily because of the sensitivity with which small changes in the temperature of the bolometer can be detected. Applications for composite high T_c bolometers exist in far infrared laboratory spectroscopy[9] and space observations of bright sources such as planets[5, 6] using radiatively cooled systems. Applications as large format infrared imagers may also exist.

Some of us have recently built composite high T_c bolometers cooled by liquid nitrogen with $D^* > 4 \times 10^9 \mathrm{cm\,Hz^{1/2}W^{-1}}$. [8, 9] The areas of these bolometers were chosen from 1 to 10 mm^2 to match the throughput of laboratory Fourier transform spectrometers. For such large areas, there are stringent requirements on thermometer sensitivity which require the use of high quality epitaxial c-axis $YBa_2Cu_3O_{7-\delta}$

(YBCO) films on favorable substrates with sharp resistive transitions and low voltage noise under current bias. Arrays of much smaller bolometers are potentially useful for thermal imaging. The absorbing area A can be as small as the diffraction limit $A = \lambda^2/\Omega$, where Ω is the solid angle of the pixel's field of view. The lower heat capacity of such small bolometers relaxes the requirement on thermometer sensitivity. The possibility then exists that YBCO on amorphous substrates like silicon nitride (Si_3N_4) could be used. Researchers at Honeywell are working on linear arrays of micromachined bolometers on substrates of Si_3N_4 membranes for thermal imaging at 10μm.[16]

This paper describes the dependence of bolometer design on area. The discussion is directly relevant to the design of imaging arrays of high T_c bolometers for wavelengths from $10 - 1000\,\mu$m. The required thermometer sensitivity for various areas will be compared with the voltage noise V_N measured for current-biased YBCO films on various substrates. We will also discuss a scheme for reading out two dimensional bolometer arrays which performs real-time signal integration on the chip.

THEORY

The voltage responsivity for a signal modulated at angular frequency ω can be written as

$$S(\omega) = \frac{IR}{G\Delta T(1+\omega^2\tau^2)^{1/2}}\,, \tag{1}$$

where I is the bias current, G is the thermal conductance to the heat sink, and τ is the thermal time constant. The temperature coefficient of resistance $dR(T)/dT = R/\Delta T$ has been written in terms of half the width ΔT of the superconducting transition, and the resistance R at the operating point near the midpoint of the transition.[1] We neglect the effects of the positive thermal feedback from the bias current I which reduces the thermal conductance to an effective value $G - I^2R/\Delta T$. To maintain

thermal stability we constrain the current by the condition

$$I^2R \leq 0.3G\Delta T. \tag{2}$$

The noise equivalent power (NEP) is calculated by summing the important sources of statistically uncorrelated noise in quadrature.

$$\text{NEP} = \left[4kT_c^2G + \frac{4kT_cR}{|S|^2} + \frac{V_N^2}{|S|^2} + \frac{e_n^2 + (i_nR)^2}{|S|^2}\right]^{1/2}. \tag{3}$$

The first term, phonon noise, in (3) is an important limit on the sensitivity of the bolometer. The last three terms, Johnson noise, excess film noise, and amplifier noise respectively, are voltage noise contributions to the NEP from the temperature read-out. In the ideal case, the responsivity S is large enough to make these terms less than or equal to the phonon noise. If these terms can be made very much less than the phonon noise for $\omega\tau \approx 1$, then the NEP can be further reduced by operating the bolometer with reduced G and $\omega\tau > 1$. The minimum heat capacity C of a practical bolometer with a given area is limited by materials and fabrication considerations. The thermal conductance G to the heat sink can be limited by the permissible temperature rise under the background power loading P, or by the required response time $\tau = C/G$, or by materials or fabrication considerations.

Our own measurements on YBCO films and those of others[17, 18] indicate that the excess voltage noise in current-biased films depends sensitively on film quality. It can be modeled as resistance fluctuations, $V_N^2 = (I\delta R)^2$, where $[\delta(\ln R)]^2$ usually has a frequency dependence between ω^{-1} and ω^{-2}, and scales roughly as the reciprocal of the film volume.[19] A resistance fluctuation δR can be written as a temperature fluctuation by using the slope of the resistive transition $\delta T = \delta(\ln R)\Delta T$. The noise equivalent temperature, NET = $\delta(\ln \text{R})\Delta\text{T}$, is introduced as a convenient figure of merit for YBCO transition-edge thermometers. The NET is the minimum temperature difference that can be measured in approximately one second of integration time.

The thermometer contribution to the NEP can then be written as

$$\mathrm{NEP_T} = \delta(\ln \mathrm{R})\Delta \mathrm{T\, G}(1+\omega^2\tau^2)^{1/2} = \mathrm{NET} \cdot \mathrm{G}(1+\omega^2\tau^2)^{1/2}. \tag{4}$$

The film noise will dominate other contributions to the readout noise if the bias current is large enough that

$$I\delta R > \left[4kT_cR + e_n^2 + (i_nR)^2\right]^{1/2}. \tag{5}$$

As will be discussed below, this condition can be met for all of the YBCO films we have measured to date without exceeding the constraint (2) set by bias heating.

Phenomena such as thermopower, Bi film resistance, gas expansion, and dielectric constant changes have been used as thermometers for thermal far-infrared detectors operating above 77 K.[20-25] For applications with frequencies less than 100 Hz, the best NET of these technologies is in the range of $10^{-6}\,\mathrm{K/Hz^{1/2}}$. If these thermometer technologies are restricted to thin films useful for large micromachined arrays,[22-26] such as bismuth films, the NET is $> 10^{-5}\,\mathrm{K/Hz^{1/2}}$. High $\mathrm{T_c}$ thin film thermometers promise values of NET $< 10^{-8}\,\mathrm{K/Hz^{1/2}}$, and hence orders of magnitude increase in detector sensitivity.

For a given optical system, the area of a pixel which couples optically to n spatial modes is proportional to the wavelength squared $A = \lambda^2 n/\Omega$. Many considerations enter the choice of the constant of proportionality n/Ω. The optical filling factor is the ratio of the area of the infrared absorber to the area of the unit cell for a single pixel (which may include other components such as charge-storage capacitors or readout circuitry). For $\lambda = 10\,\mu$m, an acceptable filling factor of (50-60%) can be achieved[26] with $A/\lambda^2 \approx 50$. Diffraction-limited pixels (n=1) with f/6 optics ($\Omega = 0.02\,$sr) and $A = 5 \times 10^{-5}\mathrm{cm}^2$ are useful at 10 μm for applications requiring high spatial resolution. Multi-mode pixels (n=10) with f/2 optics ($\Omega = 0.2\,$sr) are useful at 10μm

for applications requiring high sensitivity when detector noise-limited. The specific detectivity $D^* = A^{1/2}/\mathrm{NEP}$ is convenient for comparing detectors with different areas. We will use these concepts to discuss the sensitivity of imaging arrays of high T_c bolometers as a function of thermometer NET, bolometer area, and wavelength.

FILM PROPERTIES

Fabrication of useful high T_c composite bolometers requires films on very thin substrates to minimize heat capacity. We have chosen to study films on sapphire, silicon, and silicon nitride substrates which are strong enough to be made thin. Table I summarizes the properties of four YBCO films which were deposited by laser ablation at Conductus and Xerox. These are representative of the best performance that has been obtained to date. Samples A and B were epitaxial c-axis films deposited on crystalline substrates with buffer layers. Sample A was made *in situ* by depositing a 20 nm thick buffer layer of $SrTiO_3$ on $\{1\bar{1}02\}$ sapphire followed by 300 nm of epitaxial c-axis YBCO.[27] After breaking vacuum, silver contact pads were sputter-deposited through a shadow mask and annealed in oxygen at 500°C for 60 min. Sample B was made using a silicon substrate. A process was specifically developed to provide a pristine Si surface for epitaxial growth.[31, 32] First, a weak HF and ethanol solution was used to strip the native SiO_2 layer and to terminate the exposed silicon bonds with hydrogen. Then the Si substrate was transferred to the deposition system via a nitrogen gas-purged glove box and load-lock. The substrate was heated in vacuum to drive off the hydrogen and 40 nm of YBCO was deposited *in situ* on a 50 nm thick yttria stabilized zirconia (YSZ) buffer layer. Because of the difference in thermal expansion between silicon and YBCO, the YBCO films are under tensile stress and must be grown thinner than $\sim$ 50 nm to avoid cracking. Silver contacts were again sputter-deposited but were not annealed to avoid driving surface contaminants into

the thin YBCO film. Samples C and D were mostly c-axis YBCO deposited on amorphous Si_3N_4 films with YSZ buffer layers. The Si_3N_4 films were deposited on Si at 850°C by Low Pressure Chemical Vapor Deposition (LPCVD) at 350 mTorr using SiH_2Cl_2 and NH_3. The YBCO films were deposited by a laser ablation process similar to that used for sample A.

We measured the voltage noise with an AC-coupled, room temperature transformer and an FET amplifier. The samples were mounted on a temperature-controlled stage in a cryostat and current-biased at values typical for bolometer operation. Figure 1 shows the voltage noise for epitaxial samples A and B. The experiment was done by integrating the noise in a 2 Hz bandwidth for 15 minutes at each temperature point. The noise at the steepest part of the resistive transition for Sample A ($YBCO/SrTiO_3/Al_2O_3$) gives NET $= 3 \times 10^{-8}\,K/Hz^{1/2}$. This sample was as quiet as the best YBCO films that we have measured to date on any substrate. In general, films that satisfy other standard requirements for quality (e.g. large J_c, small ΔT) consistently show low noise before processing. Samples A and B had high critical current ($J_c > 10^6 A/cm^2$, $T = 77K$) and, as shown in Table I, narrow resistive transitions, and low resistance fluctuation noise. Processing, especially in the form of narrow, patterned lines, has been observed to increase noise. Therefore, we have avoided extensive processing of the films after deposition by using large area YBCO thermometers with the minimum resistance necessary to satisfy (5). Poor quality films tend to degrade more rapidly with processing than high quality films. At present, our yield for samples of $YBCO/SrTiO_3/Al_2O_3$ with NET $< 6 \times 10^{-8}\,K/Hz^{1/2}$ after processing is higher than 50%. After the substrate thickness of Sample A was reduced by grinding to 25μm, it was used in a composite bolometer with a sapphire substrate.[8, 9] The best NET yet obtained for YBCO on a silicon substrate is NET $= 7 \times 10^{-8} K/Hz^{1/2}$.

The resistive transitions for samples C and D of $YBCO/YSZ/Si_3N_4$ shown in Fig.

2 are significantly broader than for samples A and B and the voltage noise is higher. Consequently, the values of NET are about 100 times poorer. In general, we expect that YBCO samples with poor epitaxy make noisier thermometers. One contribution is switching noise from thermally activated flux motion. Flux can move more easily along regions of reduced energy gap parameter such as grain boundaries.[33] The frequency dependence of $\delta(\ln R)$ is determined by the distribution of activation energies for the switching processes[34] and the amplitude of $\delta(\ln R)$ depends on the number of such processes. We have strong evidence for such processes from noise measurements in an external magnetic field of both YBCO/MgO samples and YBCO/Al_2O_3 samples.[35] The YBCO/Al_2O_3 film had poorer in-plane epitaxy, as determined by x-ray analysis,[36] and higher noise, which increased with applied magnetic field. Based on experience with other substrates, we expect that the NET's for YBCO films on Si_3N_4 will improve as that technology matures.

For practical reasons, bolometers for use in large format imaging arrays must be produced by optical lithography and micromachining. Such techniques are desirable even for single bolometer elements. Our interest has focused on bolometers that consist of a high T_c thermometer and a radiation absorber such as gold black[28, 29] or a Bi film[30] deposited on a thin membrane which is isolated from the heat sink by two thin legs of the same membrane material (Fig. 3). Bolometers made on thin Si_3N_4 membranes can have very low heat capacity per unit area C_A and can be made with very low G because of the mechanical strength and the low bulk thermal conductivity of Si_3N_4. The relatively high NET of our present thermometers on Si_3N_4, however, limits the use of this substrate to relatively small bolometers with high responsivity to minimize the contribution of film noise in (4). Such bolometers are well suited, for example, to imaging arrays for $\lambda \sim 10\mu$m. Bolometers made on Si membranes have smaller values of NET, but will probably be limited to larger values of C_A

and G. They are therefore appropriate for higher throughput applications at longer wavelengths. The very low values of NET obtained on thinned sapphire substrates make this technology appropriate for very large bolometers. We will quantify this argument by calculating the dependence of the detectivity D^* on area and thus on λ for each of the above technologies using the values of NET from Table I.

The bolometer substrate technology chosen sets material limits to the heat capacity per unit area C_A that can be achieved. In addition, for the membrane technologies, there is a minimum practical value for the thermal conductance G_{min} set by the strength of the legs. If we assume that the required response time τ and the factor $A/\lambda^2 = n/\Omega$ are set by the application, then the required $G = C_A A/\tau$ will be equal to G_{min} at a specific wavelength λ_o given by

$$\lambda_o = \left(\frac{G_{min}\tau}{C_A}\frac{\Omega}{n}\right)^{1/2} . \tag{6}$$

For $\lambda < \lambda_o$, the bolometer will be faster than is required and therefore less sensitive than optimum. For $\lambda > \lambda_o$, the available range of G includes the optimum value.

We estimate C_A and G_{min} for a Si_3N_4 bolometer based on a 0.75 μm thick Si_3N_4 membrane which was built at Berkeley by other workers.[37] This membrane was supported by two Si_3N_4 legs with dimensions $0.75 \times 0.75 \times 20\,\mu$m. For a bolometer with two such legs, we calculate $G_{min} \approx 0.3\,\mu$W/K by using a handbook value for the thermal conductivity of bulk Si_3N_4 at 90 K. For a Si membrane bolometer with two undoped Si legs of the same dimensions, $G_{min} \approx 30\,\mu$W/K. From handbook data,[38] we estimate that G_{min} of doped Si legs might be roughly $0.5G_{min}$ of undoped Si legs at 90K. We expect the heat capacity of the YBCO thermometer and silver electrical contacts to dominate the substrate heat capacity, so we choose $C_A = 2.7\times10^{-5}\,\mathrm{J\,K^{-1}cm^{-2}}$ for both Si and Si_3N_4 membrane bolometers.

Figure 4 shows the prediction for D^* as a function of the normalized wavelength

λ/λ_o for a fixed value of A/λ^2 and $\tau = 10\,\mathrm{ms}$. The solid line shows the upper limit on D^* imposed by phonon noise

$$D^* = \left(\frac{A}{4kT_c^2G}\right)^{1/2}. \tag{7}$$

For $\lambda > \lambda_o$, $G \propto A$, so $D^*(\lambda)$ is constant. For $\lambda < \lambda_o$, $G = G_{min}$, so $D^*(\lambda) \propto \lambda$.

The performance of the bolometer is limited by thermometer noise if NET $> 10^{-8}\,\mathrm{K/Hz^{1/2}}$. The dashed lines show the limits on D^* from thermometer noise for various values of NET calculated from

$$D^* = \left(\frac{A}{G^2(\mathrm{NET})^2(1+\omega^2\tau^2)}\right)^{1/2}. \tag{8}$$

For $\lambda > \lambda_o$, $D^*(\lambda) \propto 1/\lambda$. For $\lambda < \lambda_o$, G is held constant at G_{min} and $D^*(\lambda) \propto \lambda$. Hence D^* peaks at $\lambda = \lambda_o$ for a pixel limited by thermometer noise. The wavelength λ_o for Si_3N_4 is 0.1 of the value of λ_o for Si since the thermal conductivity of Si_3N_4 is $\sim 1/100$ that of Si at 90K.

For a given value of A/λ^2, response time τ, and combination of YBCO thermometer and substrate, we can compute λ_o and plot the curve from Fig. 4 as D^* versus λ. Figure 5 shows this plot for $A/\lambda^2 = 50$ and $\tau = 10\,\mathrm{ms}$ for our best YBCO thermometer on both Si_3N_4 and Si membranes. For comparison, Fig. 5 also shows the performance of typical pixels in several different large format arrays operated at 77K along with the photon noise limits for photovoltaic and photoconductive detectors that view 300K radiation in a 0.02 sr field of view. The predicted performance for YBCO/YSZ/Si_3N_4, shown in Fig. 5, could be competitive with HgCdTe at $\lambda = 10\mu\mathrm{m}$ and one order of magnitude more sensitive than HgCdTe at $\lambda = 20\mu\mathrm{m}$.[39] The performance of this array at longer wavelengths is better than room temperature detectors, but is rapidly degraded by thermometer noise. An array optimized for longer wavelengths can have a better peak value of D^*. Choosing $A/\lambda^2 = 5$ and $\tau = 10\,\mathrm{ms}$, the

peak in D^* is three times higher and occurs at $\lambda = 45\,\mu$m for the same thermometer NET.

The predicted performance for a YBCO/YSZ/Si bolometer with the same assumed geometry as for Si_3N_4 is also shown in Fig. 5. The region of phonon noise limited D^* appears at longer wavelengths than for Si_3N_4 because of the higher bulk thermal conductivity of silicon. The limit to D^* from thermometer noise is higher than that of bolometers on Si_3N_4 because of the lower NET of YBCO on silicon. Arrays of high T_c bolometers on Si membranes may be useful for imaging applications for $\lambda > 20\mu$m. One example is long wavelength atmospheric imaging from NASA planetary probes such as Cassini.[5, 6]

The most important potential impact of the high T_c bolometer is in a LN cooled large format imaging array for $8 - 14\,\mu$m. This possibility depends both on the performance of the bolometer arrays as discussed above and also on the performance available from the competing HgCdTe technology. Although accurate predictions are not possible, this important question deserves further discussion. Two dimensional (2D) staring arrays for 300K thermal imaging in the atmospheric window from $8 - 14\,\mu$m require high D^* per pixel, good uniformity, and low-noise readout electronics. The predicted D^* of a high T_c bolometer used from $8 - 14\,\mu$m is worse than the D^* of a HgCdTe photovoltaic detector in a single pixel or linear array format. However, it is difficult to make 2D arrays of HgCdTe photovoltaic detectors which are larger than 128×128 pixels.[16] Even these arrays suffer from low yields and high costs. The performance of arrays of HgCdTe detectors which operate from $8 - 14\,\mu$m also suffers from high backgrounds and high leakage currents. These currents rapidly saturate the charge storage capacity of a CCD readout and can restrict the integration time of the signal.[16, 40] Many thermal imaging systems which require high spatial resolution across the field of view operate at shorter wavelengths so as to use more mature

technologies[41] with larger numbers of pixels such as PtSi[42] or InSb. Although the yield and uniformity of such arrays are excellent, the atmosphere is more opaque at these wavelengths. Also, radiation from a 300K black body is weaker at 4μm than at 10μm but stray light from visible sources such as the sun is stronger at 4μm than at 10μm. We believe large 2D arrays of high T_c bolometers on Si_3N_4 membranes will have useful sensitivity from $8 - 14\,\mu$m and could have advantages in yield and cost over large 2D arrays of HgCdTe. Without building such an array, we can not quantitatively predict the uniformity of the responsivities of pixels across the array. Equation (1) shows the uniformity in S depends only on variations in I, G, and $dR(T)/dT$. Temperature gradients across the array could produce variations in $dR(T)/dT$ from pixel to pixel. But, temperature gradients which are smaller than $\sim 0.1\Delta T$ should not seriously degrade uniformity since $R(T)$ is mostly linear on this temperature scale.

ARRAY DESIGN AND READOUT

We have predicted useful sensitivity for a single pixel high T_c bolometer with a dedicated low-frequency amplifier. Many imaging applications require large arrays of bolometers where constraints on power dissipation and filling factor only allow for a small number of amplifier channels. In simple circuits, the electrical signal from a pixel is only integrated for a tiny fraction of the observation time. The electrical noise from a pixel in an array can therefore be much greater than the noise from a single pixel with a dedicated amplifier. We now discuss a scheme which provides signal integration over the full observation time, but does not require one amplifier per pixel.

The NEP of a bolometer pixel has contributions from thermal fluctuations, including infrared source fluctuations, as well as the phonon noise, represented by the

first term in (3). It also has contributions from voltage fluctuations in the thermometer, represented by the second and third terms in (3). Thermal fluctuations occurring for $\omega_{\rm fluct}\tau \gg 1$ are integrated by the thermal response time of the bolometer. Therefore, a bolometer which operates in the source noise or phonon noise limit with τ equal to the frame time does not require additional electrical integration. In principle, however, a bolometer optimized for sensitivity has equal contributions to the NEP from both thermal fluctuations and voltage fluctuations. In practice, the bolometer designs that we have described above are sometimes limited by voltage noise fluctuations. Therefore, integration of the electrical signal is desirable.

Photovoltaic detectors in a CCD array integrate the photocurrent with a charge storage well next to each detector. Ideally, the storage capacity of the well is larger than the product of the photocurrent and the time interval between samplings by the readout amplifier. Consequently, charge fluctuations which occur faster than the sampling rate are averaged. A bolometric detector outputs a voltage equal to the product of the absorbed infrared power and the responsivity (1). An RC filter could be implemented next to the bolometer which integrates voltage fluctuations occurring on time scales shorter than RC. The RC time should approximately equal the frame time.

As a specific example, we consider a 64 × 64 imaging array of high T_c bolometers similar to existing arrays of bismuth bolometers built at Honeywell.[26] Since both the readout amplifiers and the bolometers have 1/f noise, we assume the incident radiation is chopped at 60 Hz. This leads to a frame rate of 30 Hz and a thermal time constant $\tau = 3\,\mathrm{ms}$ for each bolometer pixel. The pixels are continuously biased and dissipate less than 5μW each. The whole array is read out once while observing the target, and again while observing the chopper blade. The two frames are then digitally subtracted. Assuming four readout amplifiers, each pixel is sampled for a

maximum time $\tau_{\text{sample}} = 3\,\mu$sec. Electrical noise in the thermometer occurring at higher frequencies than 60 Hz is then aliased across the bandwidth of the readout amplifier. An RC filter next to each pixel would roll off this high frequency noise before it is aliased.

Figure 6 shows a schematic implementation of the readout circuit for a two dimensional bolometer array. The readout circuit elements could be fabricated on a separate silicon wafer which is bonded to the bolometer array with indium bumps. The R_fC filter appears in parallel with the high T_c thermometer. For conceptual simplicity, we will first consider passive circuit components. In practice, circuits with active components may consume less power and surface area. Active components are frequently used in CCD arrays.[45, 46] A polysilicon resistor with $R_f = 10\,\text{M}\Omega$ and a trench capacitor with $C = 300\text{pF}$ would give a time constant $R_fC = 3\,\text{ms}$. Typically, $R_f \gg R$ so the contribution to the NEP from Johnson noise is mostly from R_f. This contribution will be negligible if the constraint (5) is modified to

$$I\delta R > \left[4kT_cR_f + \frac{e_n^2 + (i_nR_f)^2}{f_{\text{chop}}\tau_{\text{sample}}}\right]^{1/2} . \tag{9}$$

The divisor $f_{\text{chop}}\tau_{\text{sample}}$ accounts for the reduced integration time of noise from the readout amplifier. The resulting amplifier noise contribution to the NEP is negligible for available amplifiers.[44] For example, a bolometer on a Si_3N_4 membrane using sample C could satisfy conditions (9) and (2) for $R_f = 10\text{M}\Omega$ and the array parameters described above if the YBCO is patterned into a meander line with $R = 50\text{k}\Omega$ at T_c.

It may be difficult to satisfy conditions (9) and (2) using only passive components because of size constraints on the capacitors or difficulty in making high resistance meander strips of YBCO. Although exact requirements on the anti-aliasing filter are specific to the system, we will mention two approaches for meeting the above conditions. First, the R_fC time constant could be reduced by reading out the array

more frequently. For example, most of the signal integration could be performed by a bank of larger capacitors called a frame averager which is located outside the focal plane. In this scheme, multiplexers transfer charge from a small capacitor next to a pixel to a much larger capacitor out of the focal plane at a faster rate than the chopping frequency. Then the readout amplifier samples the capacitors in the frame averager at the chopping frequency. Second, two-transistor amplifiers with anti-aliasing filters could be fabricated in silicon for each pixel. Figure 7 shows a schematic diagram of a circuit which is functionally similar to Fig. 6 but which uses active components. The depletion-mode transistor T1 presents a current bias to the bolometer without dissipating much power. The depletion-mode transistor T2 functions both as R_f for the anti-aliasing filter and as a load resistance for the common source buffer stage made from T3. This circuit has both an anti-aliasing filter and voltage gain to buffer the signal from noise in the "Select" transistor. If a specific application requires a higher resistance from the active load, a current mirror could be used in place of the depletion-mode transistor.[47] The transistors can be MOSFETs in most applications. Some applications may benefit from the lower 1/f noise of JFETs.

SUMMARY

We have discussed the optimization of high T_c bolometers for imaging arrays for wavelengths longer than $10\,\mu$m. An analysis of the thermometer sensitivity required for different pixel sizes indicates that there are useful applications for small Si_3N_4 membrane bolometers at $\lambda \sim 10\,\mu$m and larger Si membrane bolometers at longer wavelengths. A readout scheme for an array of bolometers which provides real-time signal integration on chip has also been described.

ACKNOWLEDGEMENTS

The authors gratefully acknowledge useful discussions with Paul Kruse and Matts Gustaffson. This work was supported in part by the Director, Office of Energy Research, Office of Basic Energy Sciences, Materials Sciences Division of the U.S. Department of Energy under Contract No. DE-AC03-76SF00098 (for SV, PLR), by Conductus Inc. (for KC), by the Air Force Office of Scientific Research (AFOSR) under Contract No. F49620-89-C-0017 (for DKF, THG), and by Xerox Palo Alto Research Center (for DKF). SV acknowledges a Department of Education predoctoral fellowship. DKF acknowledges an ATT predoctoral fellowship.

REFERENCES

[1] P. L. Richards, J. Clarke, R. Leoni, P. H. Lerch, S. Verghese, M. R. Beasley, T. H. Geballe, R. H. Hammond, P. Rosenthal, and S. R. Spielman, Appl. Phys. Lett. **54**, 283 (1989).

[2] P. L. Richards, S. Verghese, T. H. Geballe, S. R. Spielman, IEEE Trans. Magn. **25**, 1335 (1989).

[3] L. Xizhi, Y. Caibing, C. Xiaoneng, F. Xizeng, S. Xiangqing, L. Shuqin, X. Yizhi, Z. Bairu, Y. Caiwen, Z. Yinzi, Z. Yuying, L. Yong, W. Huisheg, S. Yinhuan, G. Ju, L. Lin, Int. J. Infrared and Millimeter Waves **10**, 445 (1989).

[4] J. C. Brasunas, S. H. Moseley, B. Lakew, R. H. Ono, D. G. McDonald, J. A. Beall, J. E. Sauvageau, J. Appl. Phys. **66**, 4551 (1989).

[5] J. C. Brasunas, S. H. Moseley, B. Lakew, R. H. Ono, D. G. McDonald, J. A. Beall, J. E. Sauvageau, SPIE Proceedings **1292**, 155 (1990).

[6] J. C. Brasunas, S. H. Moseley, B. Lakew, R. H. Ono, D. G. McDonald, J. A. Beall, J. E. Sauvageau, to appear in SPIE Proceedings **1477**, (1991).

[7] B. Dwir, L. Pavesi, J. H. James, B. Kellett, D. Pavuna, F. K. Reinhart, Supercond. Sci. Technol. **2**, 314 (1989).

[8] S. Verghese, P. L. Richards, K. Char, S. A. Sachtjen, SPIE Proceedings **1292**, 137 (1990).

[9] S. Verghese, P. L. Richards, K. Char, S. A. Sachtjen, IEEE Trans. Magn. **27**, 3077 (1991).

[10] G. L. Carr, M. Quijada, D. B. Tanner, C. J. Hirschmugl, G. P. Williams, S. Etemad, B. Dutta, F. DeRosa, A. Inam, T. Venkatesan, X. Xi, Appl. Phys. Lett. **57**, 2725 (1990).

[11] W. S. Brocklesby, D. Monroe, A. F. J. Levi, M. Hong, S. H. Liou, J. Kwo, C. E. Rice, P. M. Mankiewich, R. E. Howard, Appl. Phys. Lett. **54**, 1175 (1989).

[12] J. G. Forrester, M. Gottlieb, J. R. Gavaler, A. I. Braginski, Appl. Phys. Lett. **53**, 1332 (1988).

[13] H. S. Kwok, J. P. Zheng, Q. Y. Ying, Appl. Phys. Lett. **54**, 2473 (1989).

[14] Qing Hu, P. L. Richards, Appl. Phys. Lett. **55**, 2444 (1989).

[15] M. Nahum, Qing Hu, P. L. Richards, IEEE Trans. Magn. **27**, 3081 1991.

[16] T. G. Stratton, B. E. Cole, P. W. Kruse, R. A. Wood, SC Global 90 International Superconductor Applications Convention Proc., CA Jan., (1990).

[17] P. Rosenthal, R. H. Hammond, M. R. Beasley, R. Leoni, P. Lerch, J. Clarke, IEEE Trans. Magn. **25**, 973 (1989).

[18] R. C. Lacoe, J. P. Hurrell, K. Springer, I. D. Raistrick, R. Hu, J. F. Burch, R. S. Simon, IEEE Trans. Magn. **27**, 2832 (1991).

[19] F. N. Hooge, A. M. H. Hoppenbrouwers, Physica **45**, 386 (1969).

[20] See, for example, the Barnes thermopile detector, EDO Corp., Shelton, Ct.

[21] T. L. Hwang, S. E. Schwarz, D. B. Rutledge, Appl. Phys. Lett. **34**, 773 (1978).

[22] D. P. Neikirk, W. W. Lam, D. B. Rutledge, Int. J. Infrared Millimeter Waves **5**, 245 (1984).

[23] T. W. Kenny, W. J. Kaiser, S. B. Waltman, J. K. Reynolds, submitted to Appl. Phys. Lett.

[24] M. J. E. Golay, Rev. Sci. Inst. **20**, 816 (1949).

[25] See, for example, the P-41 detector, Molectron Corp., Sunnyvale, CA.

[26] P. W. Kruse (private communication).

[27] K. Char, N. Newman, S. M. Garrison, R. W. Barton, R. C. Taber, S. S. Laderman, R. D. Jacowitz, Appl. Phys. Lett. **57**, 409 (1990).

[28] L. Harris, J. K. Beasley, J. Opt. Soc. **42**, 134 (1952).

[29] L. Harris, J. Opt. Soc. **51**, 80 (1960).

[30] J. Clarke, G. I. Hoffer, P. L. Richards, N-H. Yeh, J. Appl. Phys. **48**, 4865 (1977).

[31] D. K. Fork, D. B. Fenner, R. W. Barton, J. M. Phillips. G. A. N. Connell, J. B. Boyce, T. H. Geballe, Appl. Phys. Lett. **57**, 1161 (1990).

[32] D. K. Fork, A. Barrera, T. H. Geballe, A. M. Viano, D. B. Fenner, Appl. Phys. Lett. **57**, 2504 (1990).

[33] M. J. Ferrari, M. Johnson, F. C. Wellstood, J. Clarke, D. Mitzi, P. A. Rosenthal, C. B. Eom, T. H. Geballe, A. Kapitulnik, M. R. Beasley, Phys. Rev. Lett. **64**, 72 (1990).

[34] P. Dutta, P. M. Horn, Rev. Mod. Phys. **53**, 497 (1981).

[35] S. Verghese, P. L. Richards, K. Char, S. M Garrison, R. W. Barton, unpublished.

[36] K. Char, D. K. Fork, T. H. Geballe, S. S. Laderman, R. C. Taber, R. D. Jacowitz, F. Bridges, G. A. N. Connell, J. B. Boyce, Appl. Phys. Lett. **56**, 785 (1990).

[37] Matts Gustaffson (private communication).

[38] Y. S. Touloukian, *Thermophysical Properties of Matter: Thermal Conductivity of Metallic Elements and Alloys*, (IFI/Plenum, New York, 1970), p.326.

[39] Eric R. Fossum, Innovative Long Wavelength Infrared Detector Workshop, JPL, April 24 (1990).

[40] A. Rogalski, J. Piotrowski, Progress in Quantum Electronics, **12**, 87 (1988).

[41] P. R. Norton, initially submitted to IEEE Trans. Elect. Dev., resubmitted to Optical Engineering.

[42] J. Mooney (private communication).

[43] W. K. Shubert, Sandia Tech. Report, **Sand84**, 2022 (1984).

[44] An amplifier built with a Toshiba 2SK137 JFET input stage can have a noise temperature of 100 mK at frequencies lower than 100 Hz with $\sim$ 10MΩ noise resistance.

[45] M. B. Reine, Innovative Long Wavelength Infrared Detector Workshop, JPL, April 24 (1990).

[46] N. Bluzer, A. S. Jensen, Optical Engineering **26**, 241 (1987).

[47] P. R. Gray, R. G. Meyer, *Analysis and Design of Analog Integrated Circuits*, (John Wiley, New York, 1984), p.710.

FIGURE CAPTIONS

Figure 1. Resistance and voltage noise at 10 Hz in current biased YBCO films measured as a function of temperature. The noise in the measurement system is 0.15 $nV/Hz^{1/2}$. Sample A is 300 nm of epitaxial YBCO on a 20 nm buffer layer of $SrTiO_3$ on sapphire. Sample B is 40 nm of epitaxial YBCO on a 50 nm buffer layer of yttria-stabilized zirconia on silicon.

Figure 2. Resistance and voltage noise at 10 Hz in current biased YBCO films measured as a function of temperature. The noise in the measurement system is 0.15 $nV/Hz^{1/2}$. Sample C is 300 nm YBCO on a 20 nm buffer layer of yttria-stabilized zirconia on Si_3N_4. Sample D is 40 nm YBCO on a 50 nm buffer layer of yttria-stabilized zirconia on Si_3N_4.

Figure 3. Diagram of a membrane bolometer. The bolometer consists of a radiation absorber and a YBCO thermometer deposited on a membrane of Si or Si_3N_4 which is isolated from the heat sink by two thin legs.

Figure 4. Specific detectivity D^* as a function of reduced wavelength λ/λ_o where λ_o depends on the minimum achievable values of the heat capacity per unit area C_A and thermal conductance G_{min} as well as the response time τ. the number n of electromagnetic modes which couple, and the solid angle Ω of the pixel's field of view. The solid line shows the predicted phonon noise limit for a bolometer on a thin membrane. The dashed lines show upper limits on D^* for thermometers with various values of NET.

Figure 5. Specific detectivity D^* as a function of wavelength for diffraction-limited pixels with $\Omega = 0.02\,\mathrm{sr}$ (f/6 optics) and $\tau = 10\,\mathrm{ms}$. The thick lines show the predicted

D^* for high T_c bolometers on silicon and Si_3N_4 membranes using YBCO thermometers. These lines were calculated using estimates for the minimum achievable heat capacity and thermal conductance and using measurements of voltage noise in high T_c thermometers. Typical values of D^* for InSb, PtSi, and HgCdTe detectors in two dimensional staring arrays operated at 77K are shown for comparison. Also shown are the photon noise limits for photovoltaic and photoconductive detectors which view 300K radiation in a 0.02 sr field of view.

Figure 6. Schematic layout of a possible implementation of a high T_c bolometer array with a novel readout scheme in which above-band electrical noise from each pixel is integrated by an R_fC filter. In this scheme, a multiplexed readout amplifier which undersamples a given pixel does not alias above-band noise into the signal channel. The unit cell consists of a YBCO thermometer R, an R_fC filter, an access transistor, a load resistor R_L, and bias lines. The voltage across R appears on the appropriate "READ" line when the "SELECT" voltage is high. All pixels are constantly under bias. The readout circuit elements would be implemented on a separate Si wafer which could be indium bump-bonded to the bolometer pixels. The optical fill factor will probably be limited by geometrical constraints on the bolometer imposed by requirements for thermal isolation.

Figure 7. Schematic layout of a readout for a single pixel which is functionally similar to a single cell in Fig. 6 but uses active devices. This circuit has both an anti-aliasing filter and voltage gain to buffer the signal from noise in the "Select" transistor. The power consumption and size of this circuit can be much smaller than the circuit shown in Fig. 6.

Table 1. Characteristics of YBCO films measured for use as thermometers on high T_c bolometers.

Sample	Source	Geometry	$\left(\frac{1}{R}\frac{dR}{dT}\right)^{-1}$ (K)	δ (ln R) ($Hz^{-1/2}$)	NET (K $Hz^{-1/2}$)	ρ_{DC} ($\mu\Omega$cm) at midpoint
A	Conductus	1 x 1 mm^2 300 nm YBCO/20 nm $SrTiO_3/Al_2O_3$	1	$3 \cdot 10^{-8}$	$3 \cdot 10^{-8}$	37
B	Xerox	1 x 3 mm^2 40 nm YBCO/50 nm YSZ/Si	2.6	$3 \cdot 10^{-8}$	$8 \cdot 10^{-8}$	55
C	Conductus	3 x 3 mm^2 300 nm YBCO/20 nm YSZ/Si_3N_4	6	$4 \cdot 10^{-7}$	$2.4 \cdot 10^{-6}$	270
D	Xerox	1 x 3 mm^2 40 nm YBCO/50 nm YSZ/Si_3N_4	5	10^{-6}	$5 \cdot 10^{-6}$	190

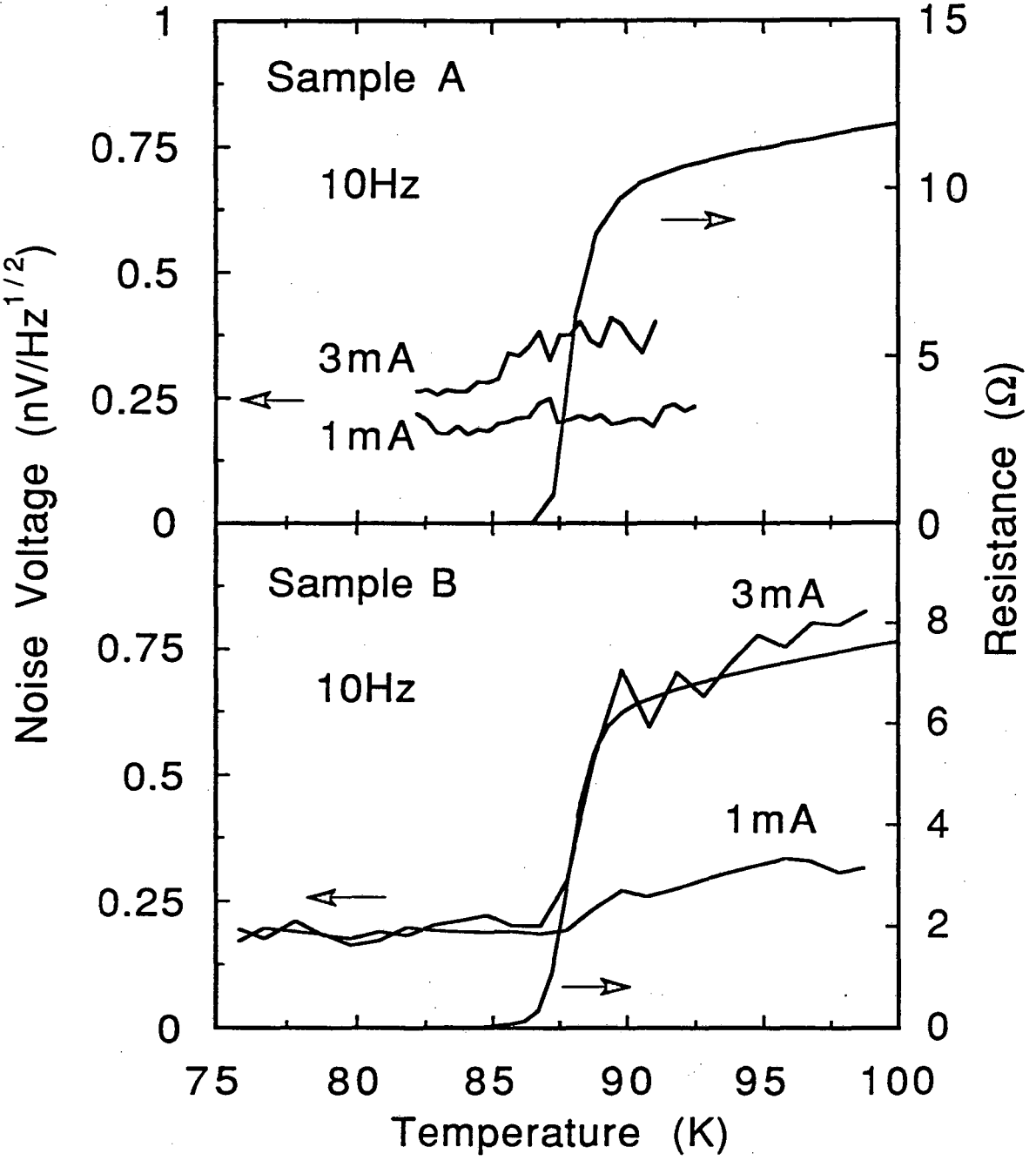

XBL 917-1400

FIGURE 1

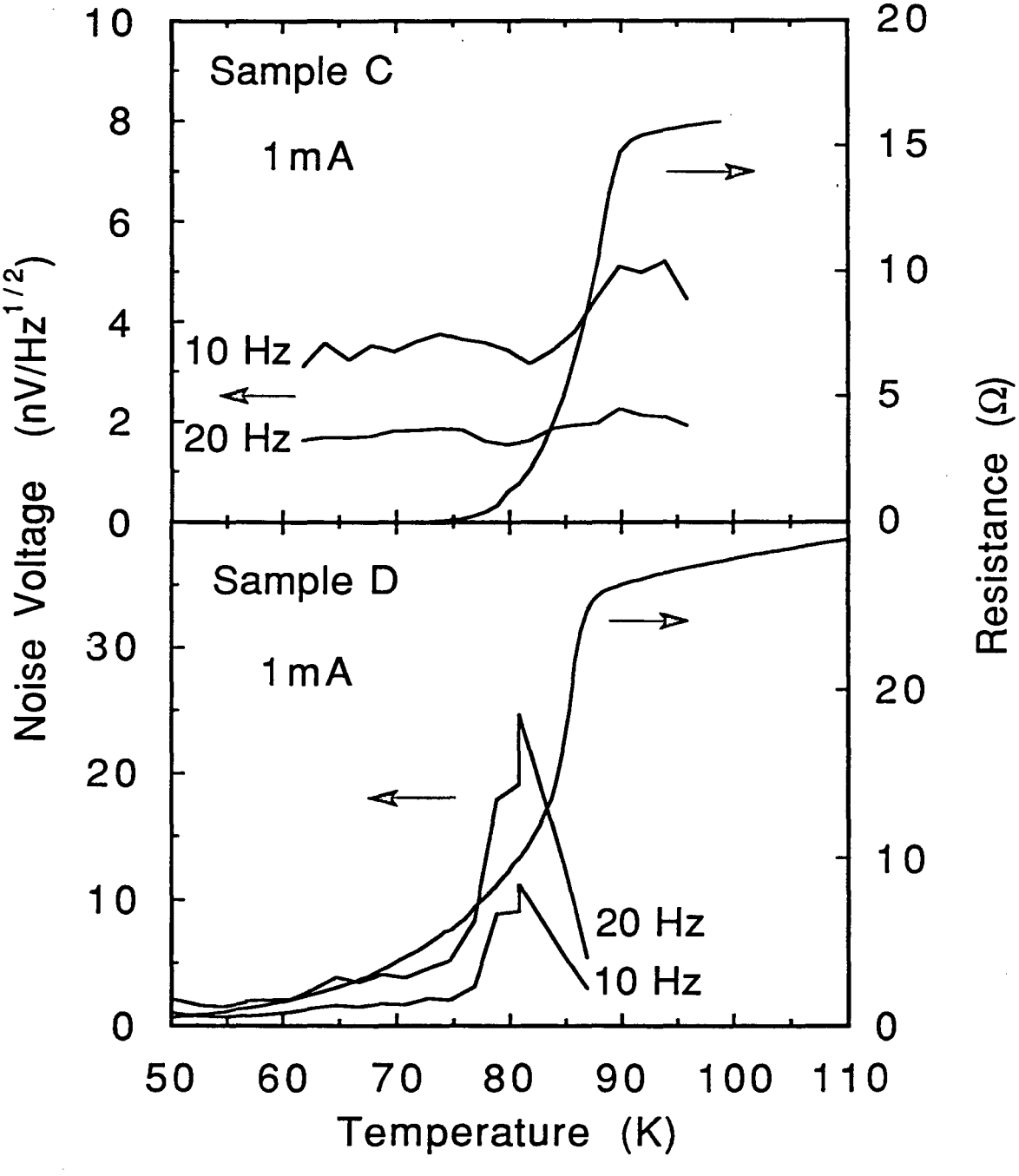

XBL 917-1401

FIGURE 2

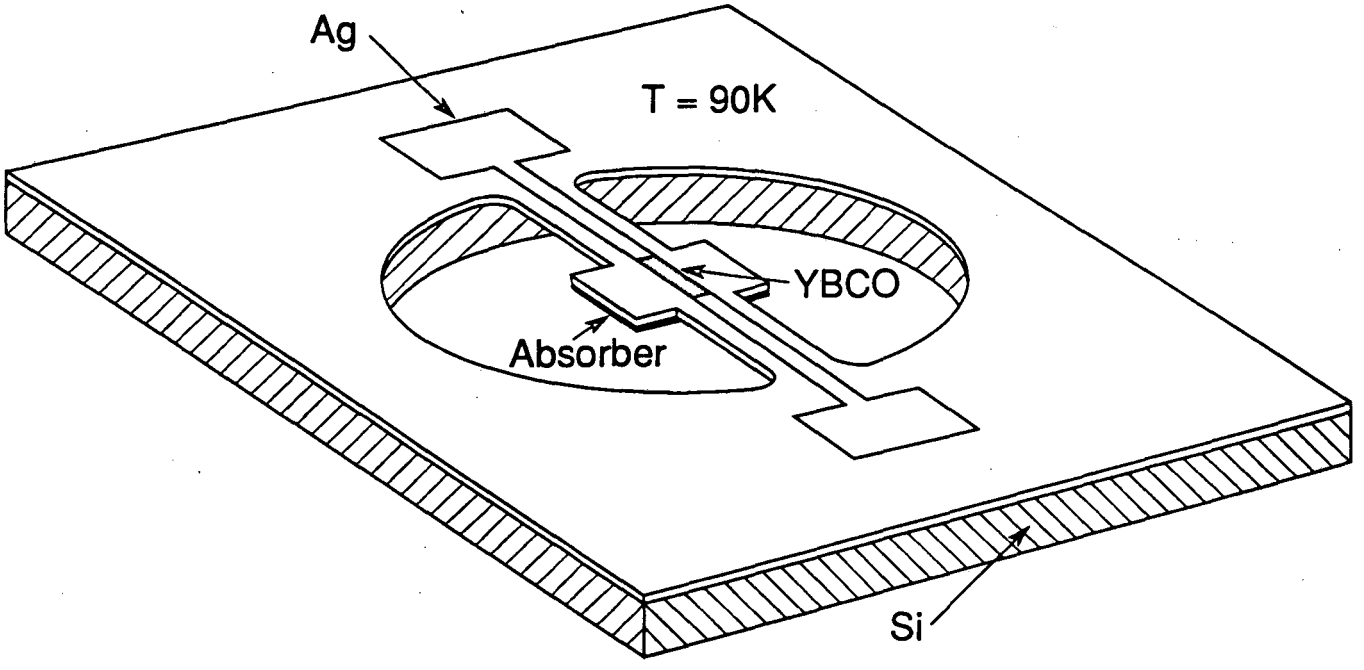

XBL 915-4831

FIGURE 3

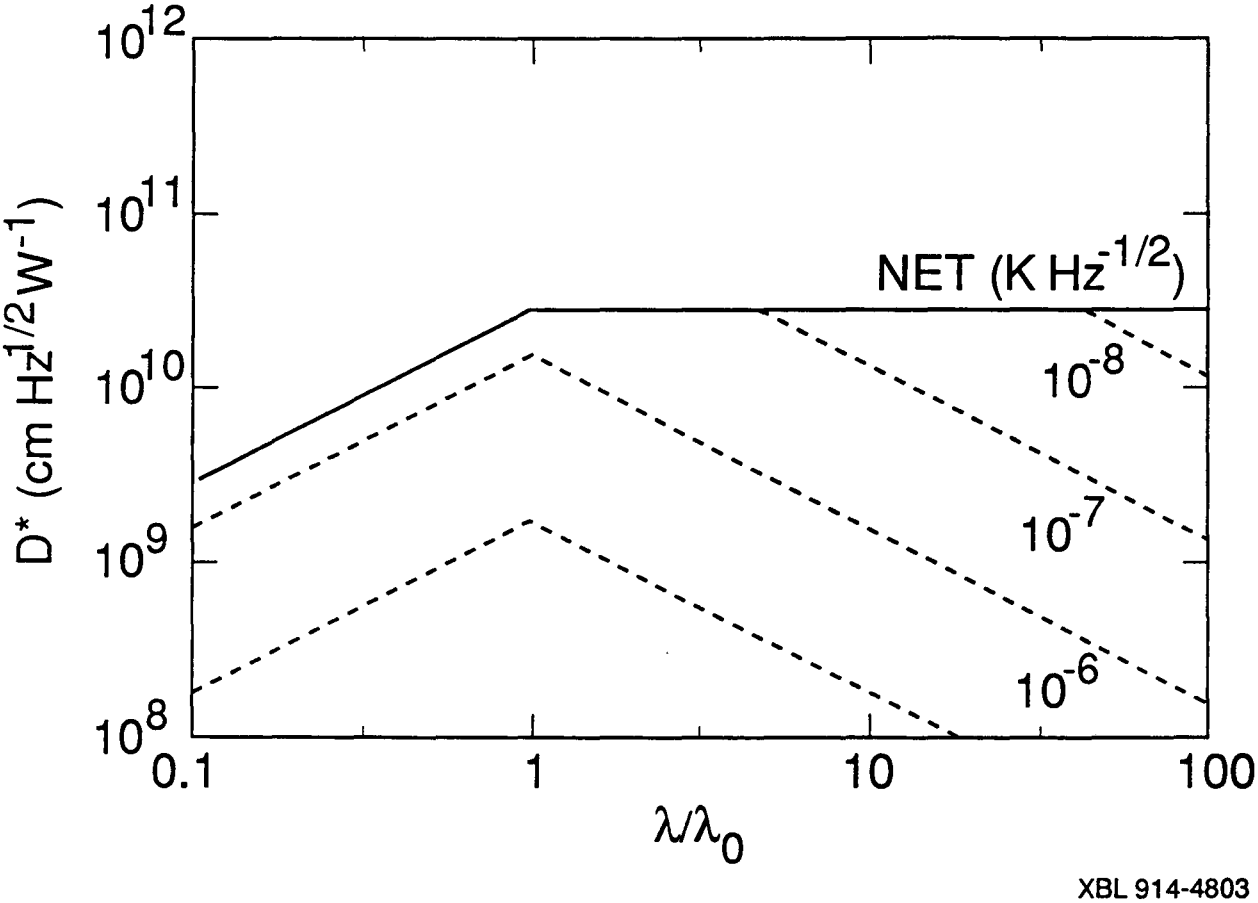
10^{12}
10^{11}
10^{10}
10^{9}
10^{8}
D* (cm $Hz^{1/2}W^{-1}$)
NET (K $Hz^{-1/2}$)
10^{-8}
10^{-7}
10^{-6}
0.1
1
10
100
λ/λ_0
XBL 914-4803

FIGURE 4

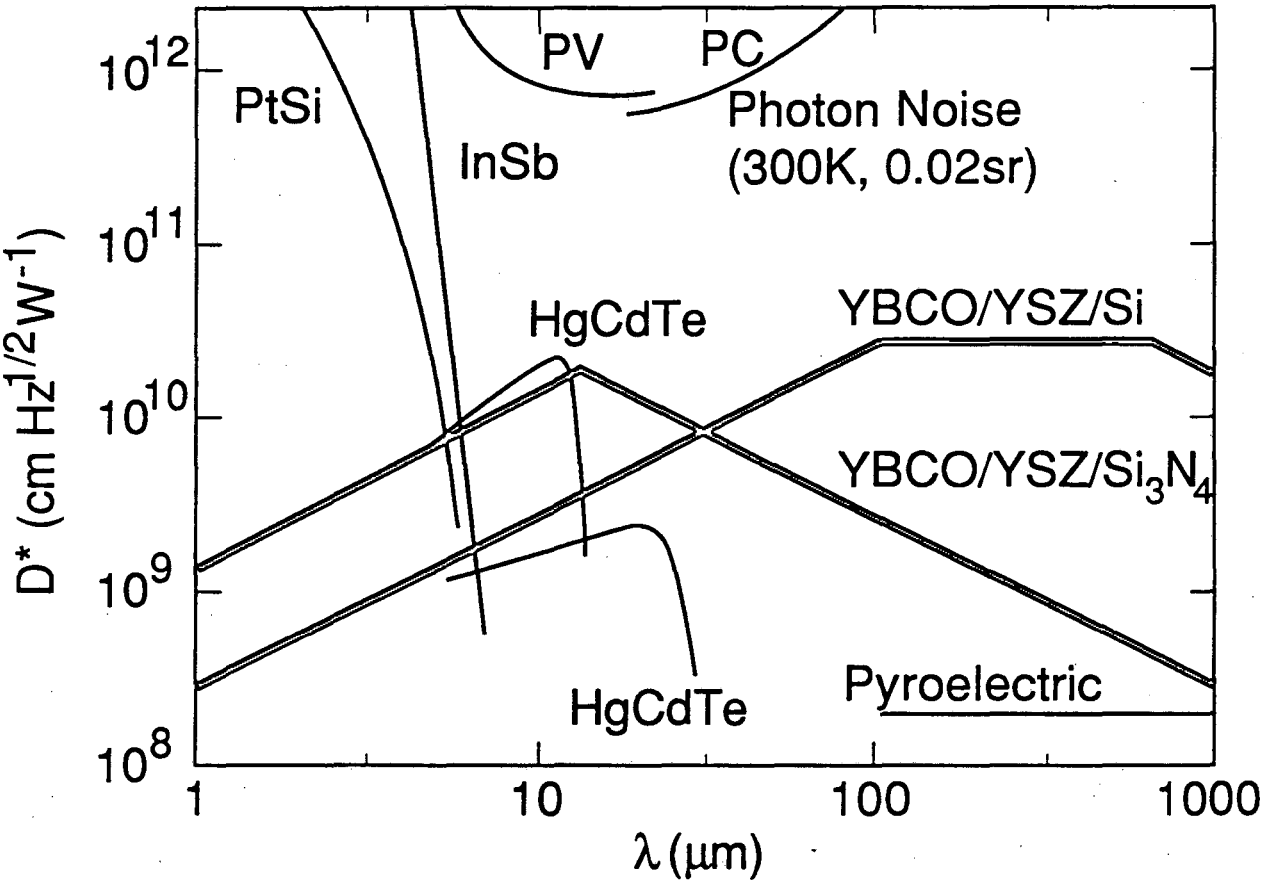

XBL 914-4802

FIGURE 5

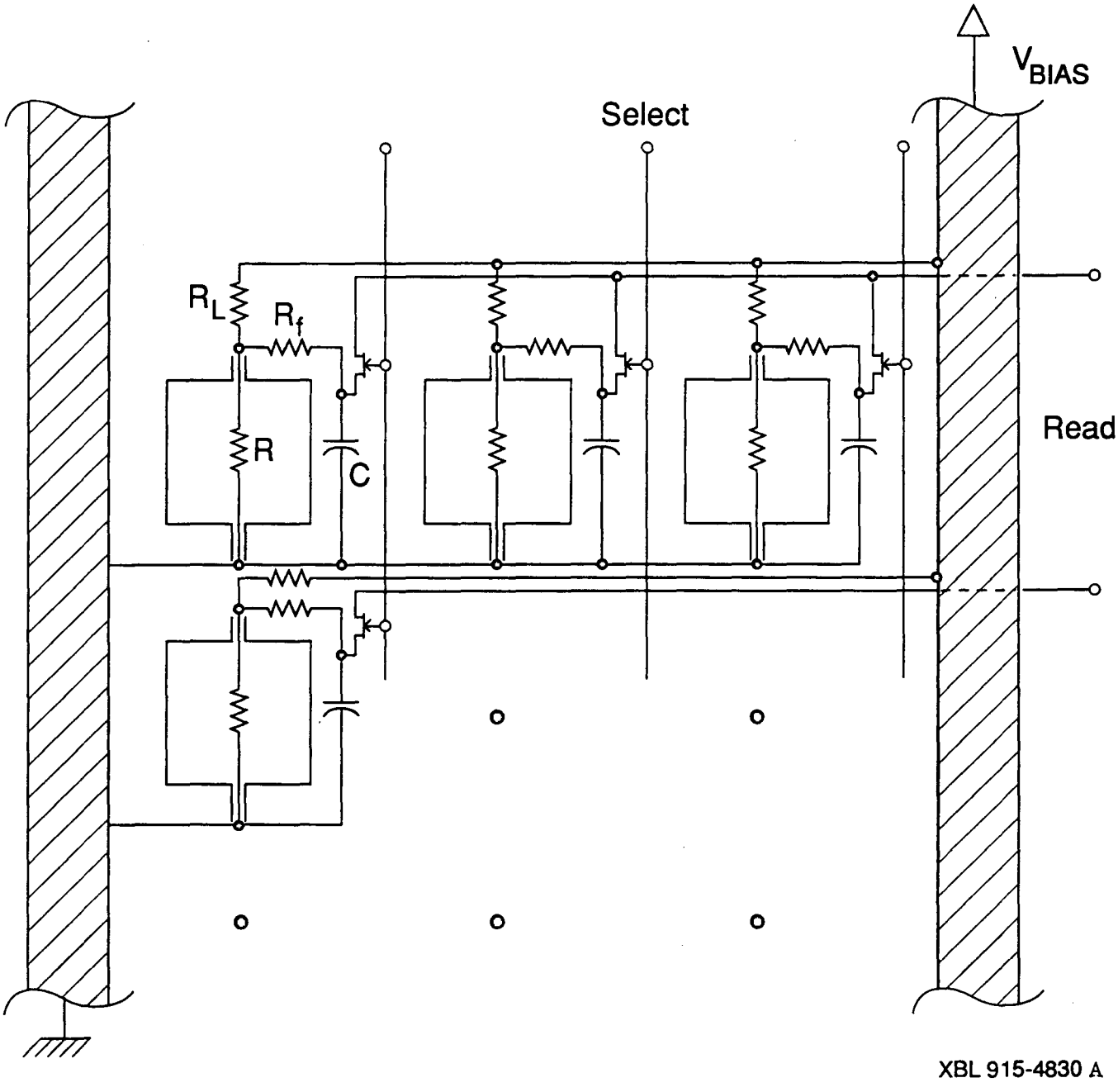

FIGURE 6

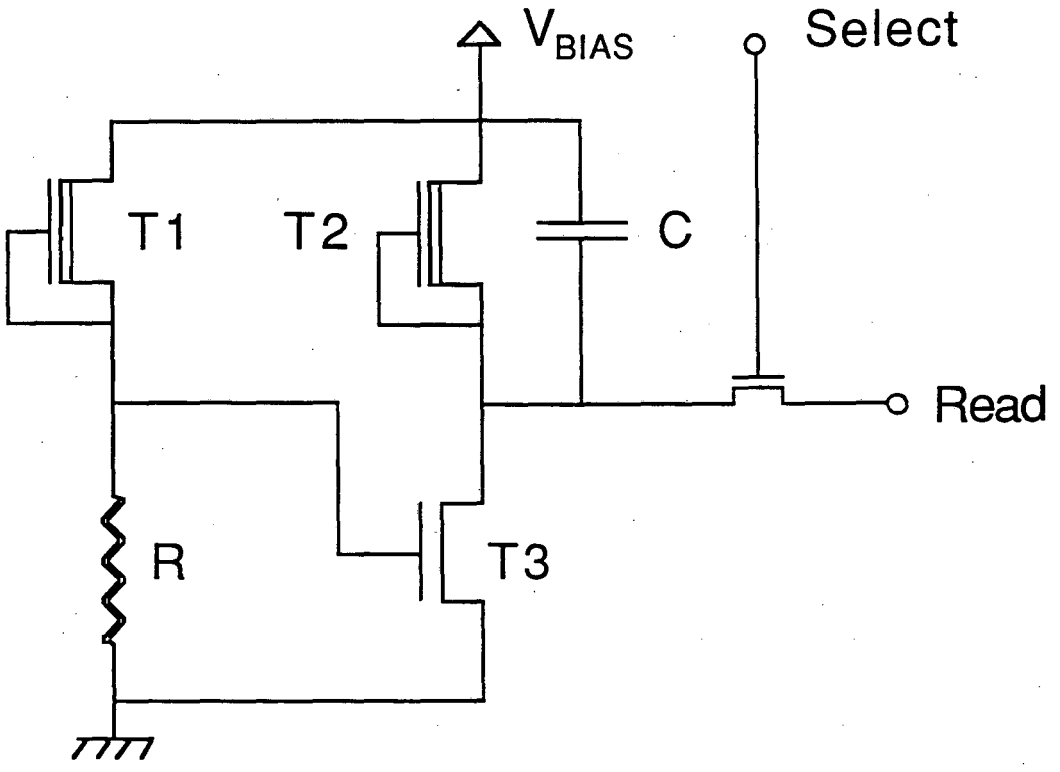

XBL 9110-4983

FIGURE 7

LAWRENCE BERKELEY LABORATORY
CENTER FOR ADVANCED MATERIALS
1 CYCLOTRON ROAD
BERKELEY, CALIFORNIA 94720